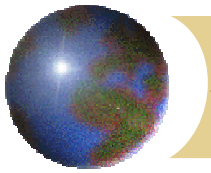


Modeling Radiation Belt Electrons

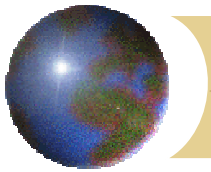
Kristi A. Keller, Mei-Ching Fok, Ayrís Falasca, Michael Hesse, Lutz Rastaetter, Maria M. Kuznetsova
NASA Goddard Space Flight Center

Tamas I. Gombosi, Darren L. DeZeeuw
University of Michigan



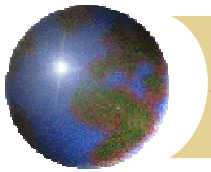
BATSRUS Information

- BATSRUS solves the ideal MHD equations using an adaptive mesh. In this run the smallest resolution was $1/8 R_E$. After the initial setup, the grid was fixed.
- The box was from -255 to $33 R_E$ in the GSM x direction and -48 to $48 R_E$ in the other two directions.
- The FACs at $4 R_E$ are mapped along dipole field lines to the ionosphere to calculate the electrostatic potential in the ionosphere.



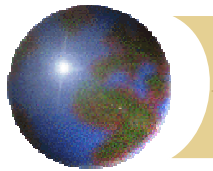
Fok Model

- ✚ The Fok Radiation Belt and Ring Current Models calculate the evolution of the ring current particle fluxes by solving a bounce-averaged Boltzmann transport equation.
- ✚ The model uses a combined drift-diffusion approach.
 - ▣ The particle drift terms include gradient-curvature drift and $E \times B$ drift (includes corotation and the ionospheric electric field).
 - ▣ The diffusion term is radial diffusion.



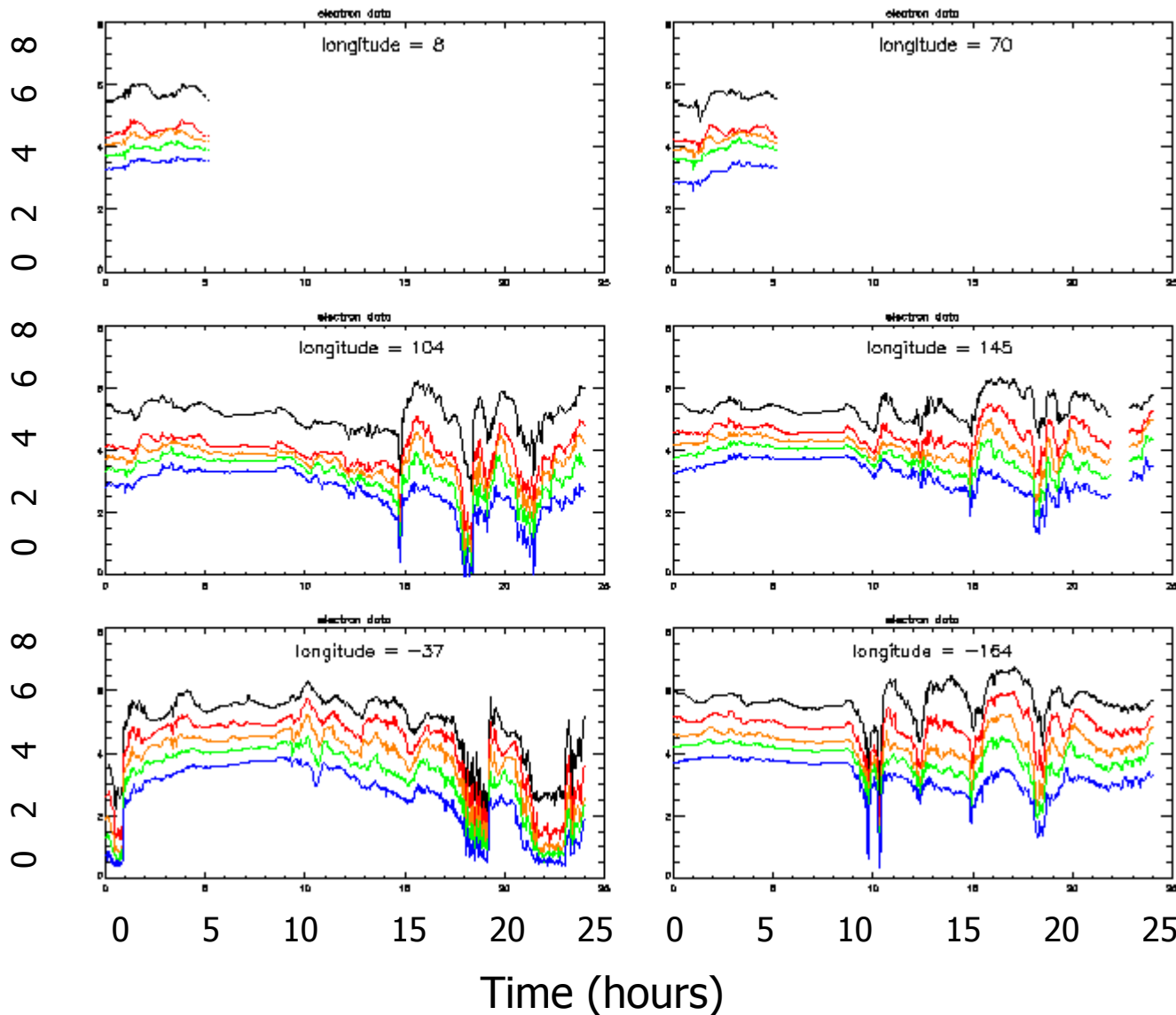
Fok Model

- The Fok Radiation Belt and Ring Current Models use the ionospheric potential and magnetic field from the BATSRUS model.
- The Fok Ring Current Model uses the density and temperature from the BATSRUS model at the Ring Current Model's outer boundary.
- The Fok Radiation Belt Model can either use the density and temperature from the MHD model or use an empirical formula to calculate a uniform density and temperature for the boundary.
- The pitch-angle distribution at the model's outer boundary is assumed to be isotropic.
- For the initial source population, the energy distribution is assumed to be a Kappa distribution.



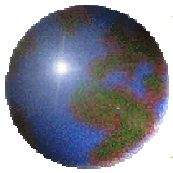
April 19, 2002 LANL Data

Log(Electron Flux ($\#/cm^2/s/sr/keV$))

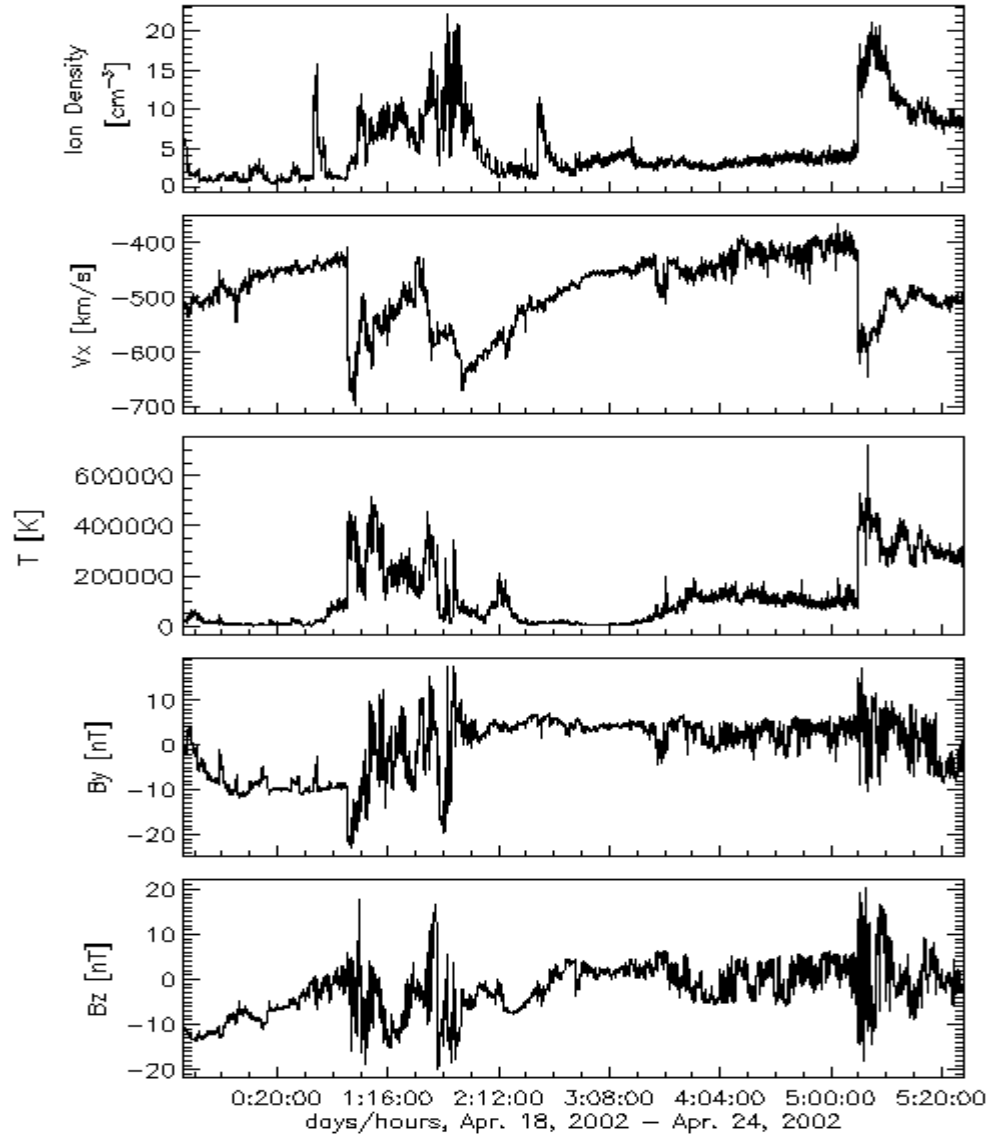


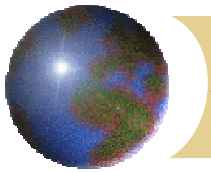
Black: 50-75keV
Red: 75-105keV
Orange: 105-150keV
Green: 150-225keV
Blue: 225-315keV

Geosynchronous electron flux data was provided by the Energetic Particle team at Los Alamos National Laboratory, Richard Belian (PI).



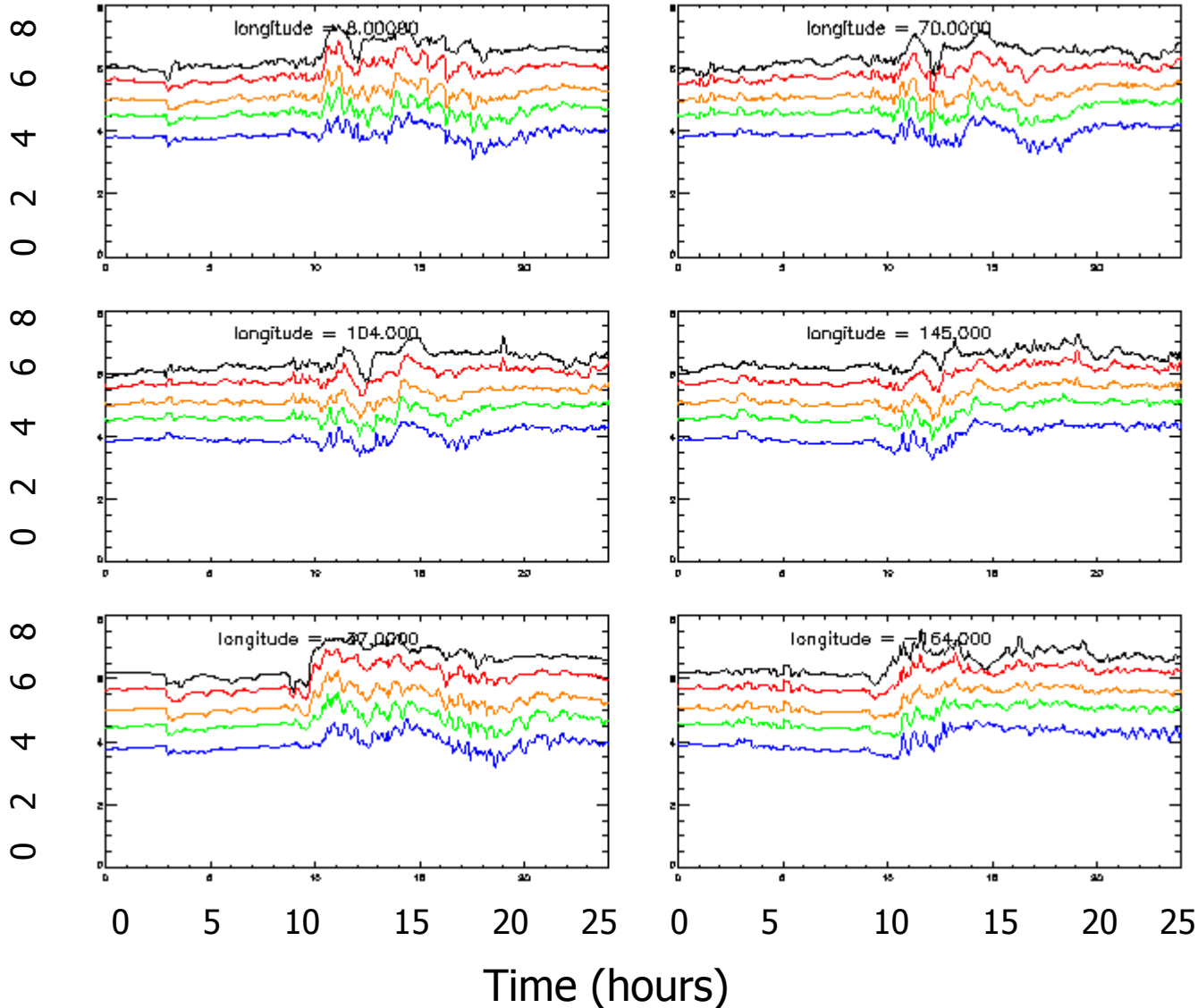
Solar Wind Data April 18-24, 2002





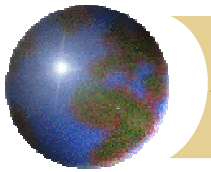
Model Results for April 19

Log(Electron Flux (#/cm²/s/sr/keV))



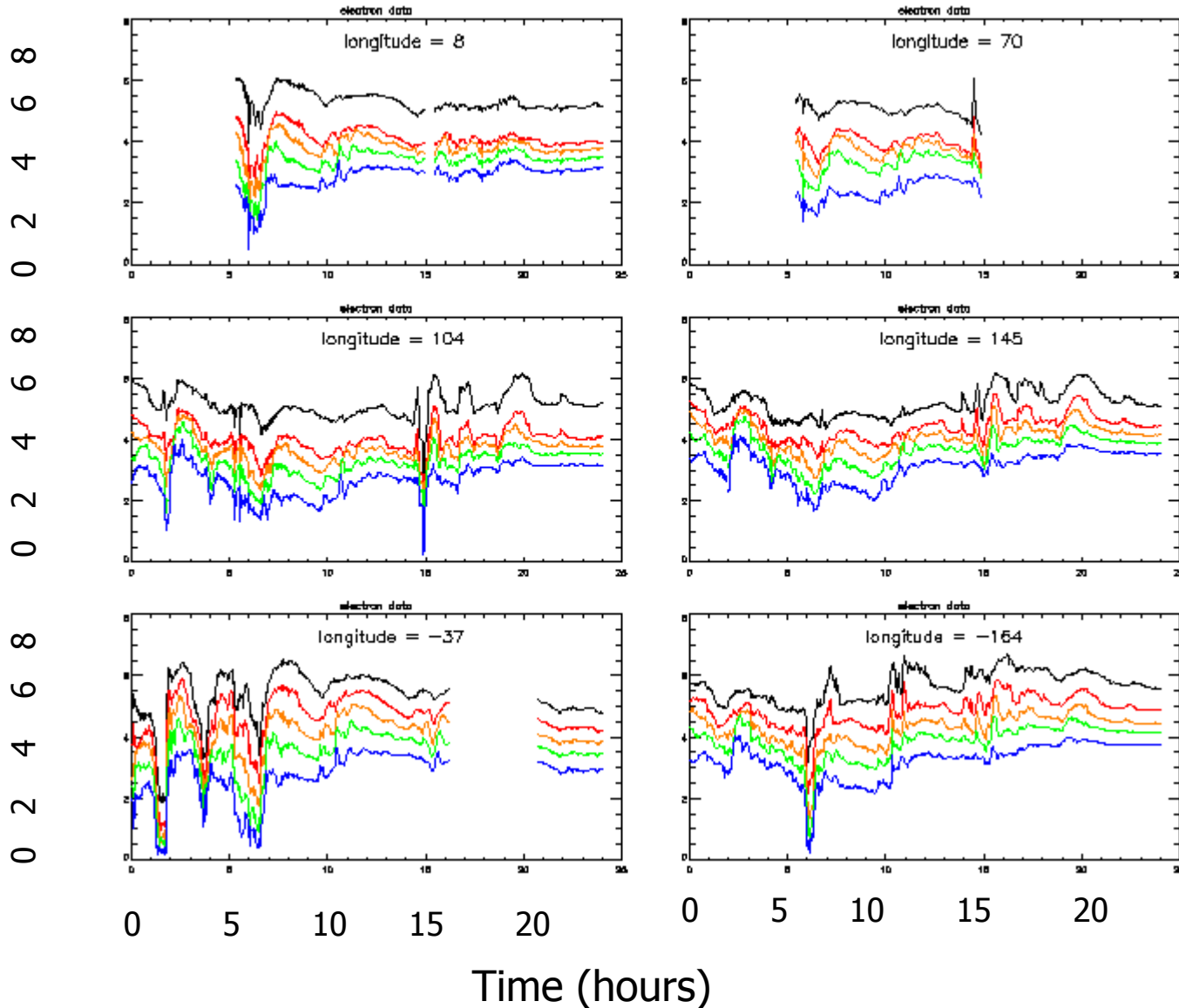
Black: 62.5 keV
Red: 90 keV
Orange: 137.5 keV
Green: 187.5 keV
Blue: 270 keV

Ring Current Model



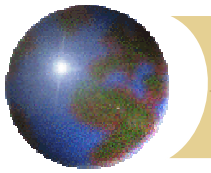
April 20, 2002 LANL Data

Log(Electron Flux (#/cm²/s/sr/keV))



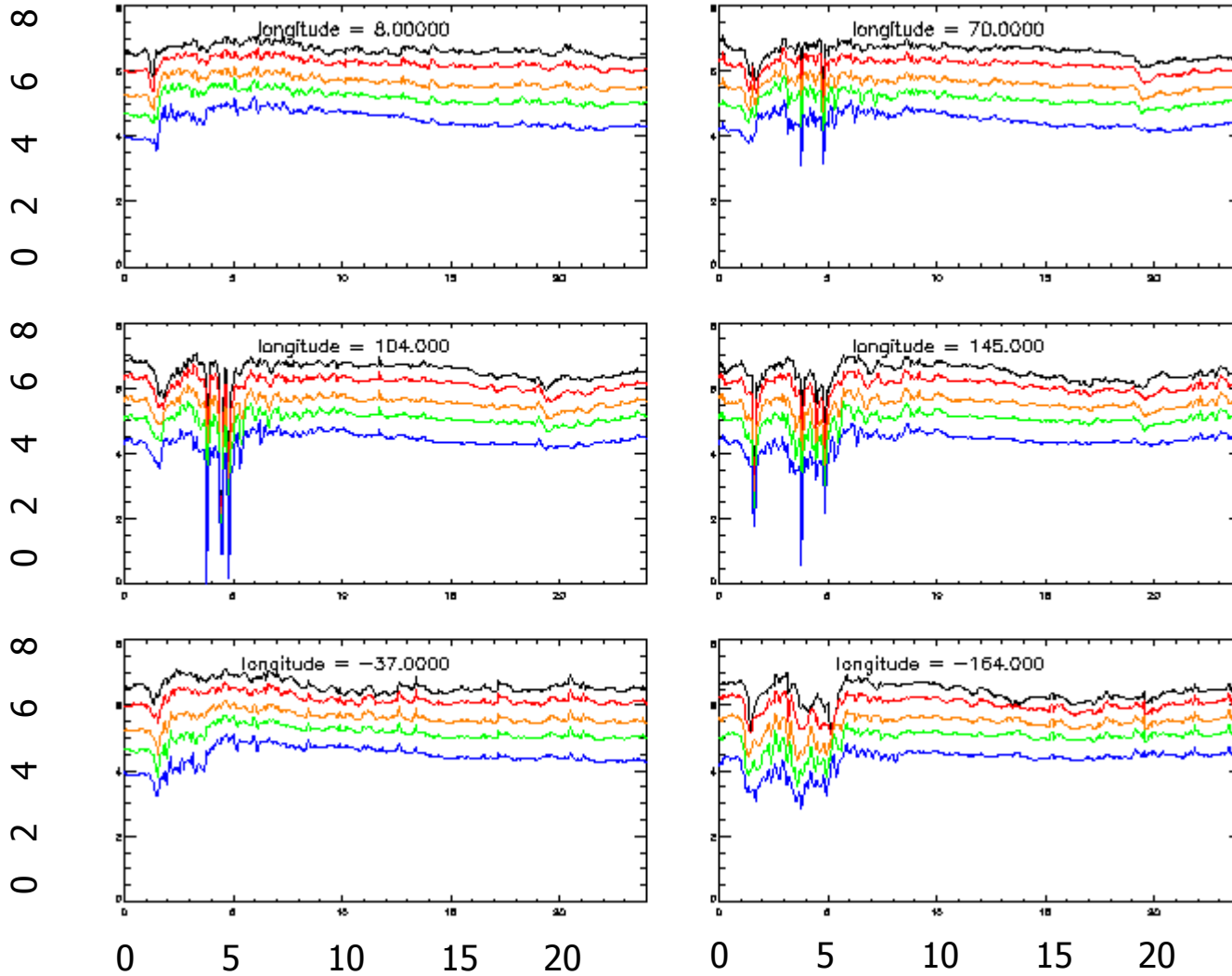
Black: 50-75keV
Red: 75-105keV
Orange: 105-150keV
Green: 150-225keV
Blue: 225-315keV

Geosynchronous electron flux data was provided by the Energetic Particle team at Los Alamos National Laboratory, Richard Belian (PI).



Model Results for April 20

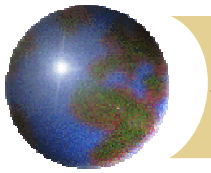
Log(Electron Flux (#/cm²/s/sr/keV))



Black: 62.5 keV
Red: 90 keV
Orange: 137.5 keV
Green: 187.5 keV
Blue: 270 keV

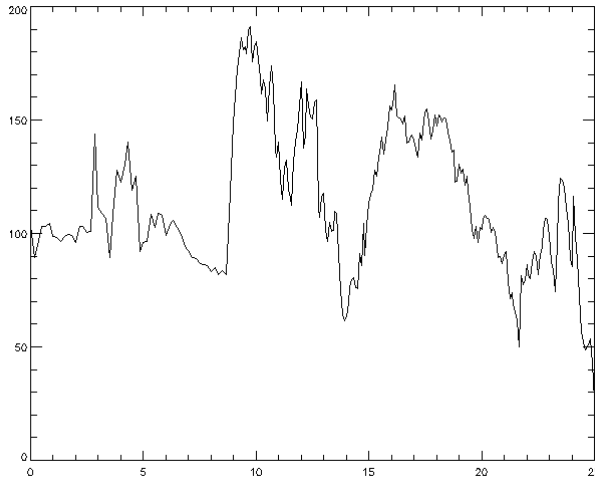
Time (hours)

Ring Current Model



Cross Polar Cap Potential

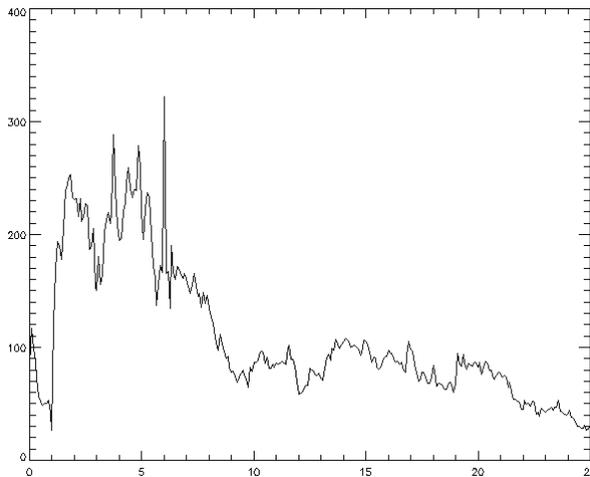
Potential (kV)



April 19

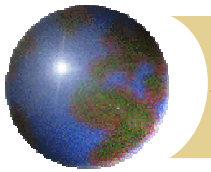
Most of the activity seen in the ring current model is associated with changes in the ionospheric potential.

Potential (kV)



April 20

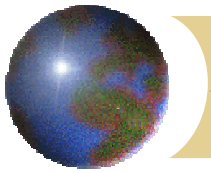
Time (Hours)



Model and Data Comparison

Magnitude Comparison

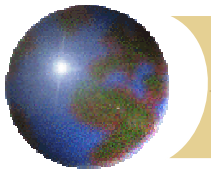
- The model flux results typically range in magnitude:
 - 62.5 keV: $10^6 - 10^7$
 - 90 keV: $10^{5.5} - 10^{6.5}$
 - 137.5 keV: $10^{4.5} - 10^6$
 - 187.5 keV: $10^{4.5} - 10^{5.5}$
 - 270 keV: $10^4 - 10^5$
- The data flux results typically range in magnitude:
 - 50-75 keV: $10^{4.5} - 10^6$
 - 75-105 keV: $10^4 - 10^5$
 - 105-150 keV: $10^4 - 10^5$
 - 150-225 keV: $10^{2.5} - 10^4$
 - 225-315 keV: $10^2 - 10^{3.5}$
- The model results tend to be higher in flux than the data. This corresponds to the density being too high at the boundary.
- Both have approximately 2.5 order of magnitude spread in flux levels from the highest energy (blue) bin to the lowest energy (black) bin shown in the plots. This corresponds to getting the mean energy about right.



Model and Data Comparison

Fluctuations

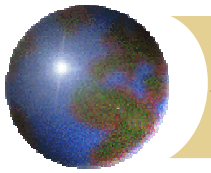
- Both model and data show very little fluctuations for the little activity for the first 10 hours of April 19. Both model and data show more fluctuations after 10 hours. The model shows more activity and the magnitude of the fluctuations are significantly higher for the data.
- For April 20, the model shows some activity for the first 5 hours but is quiet for the remainder of the day. There is more activity in the data and it lasts most of the day.



Model and Data Comparison

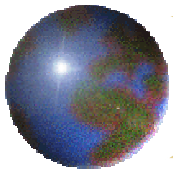
Features seen in the data and missing in the model results for this event

- Large magnitude dispersionless injections
 - April 19 15:00
- Flux dropouts
 - April 20 1:00 - 2:00
- Long-term flux decreases
 - April 20 2:00 – 5:00

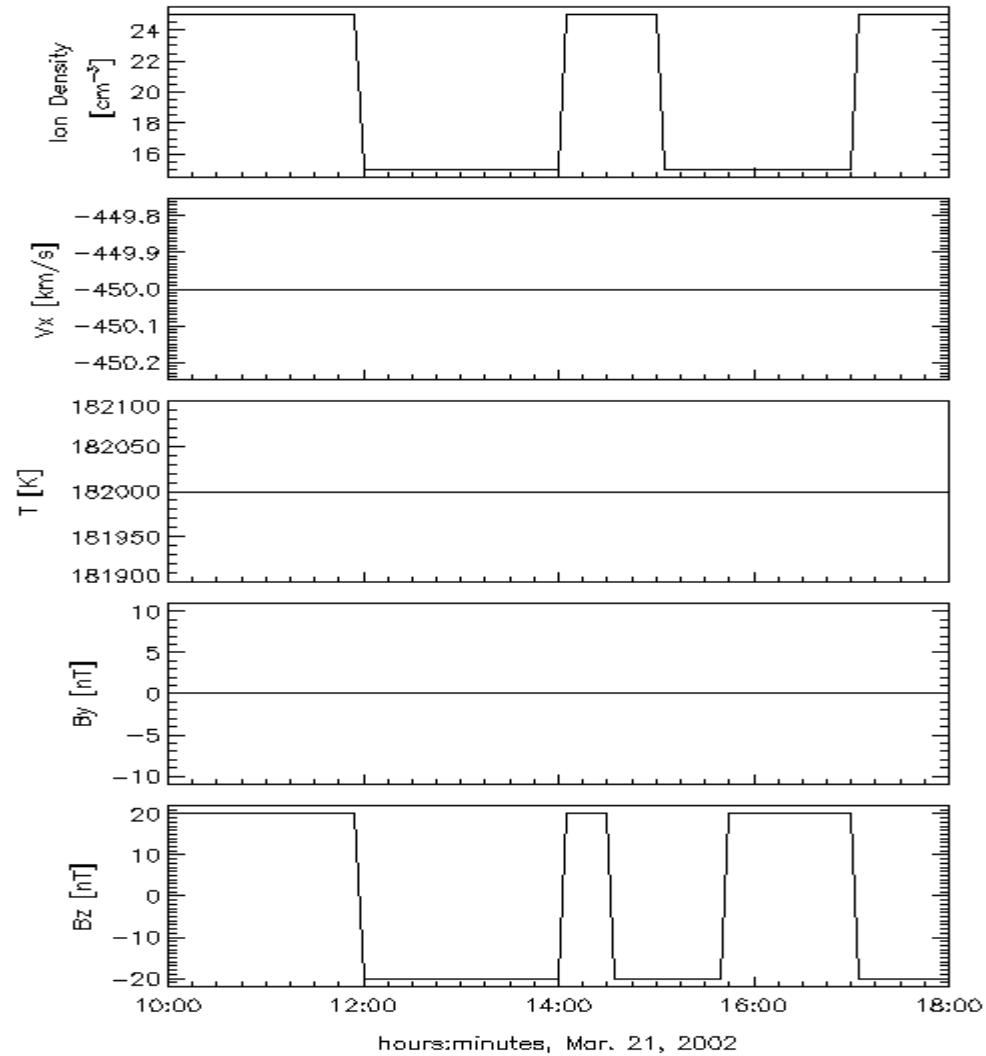


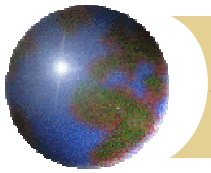
Other Cases

- ❖ In simulated solar wind runs, we have seen dispersionless injections and flux dropouts. The flux dropouts are more apparent in the simulation of protons than for electrons.
- ❖ The dropouts and dispersionless injections occur when there is magnetic field stretching in the tail followed by reconnection.
- ❖ The flux dropouts are shorter duration than the examples seen in the April event. The tail stretching is on a time span of 20 minutes.



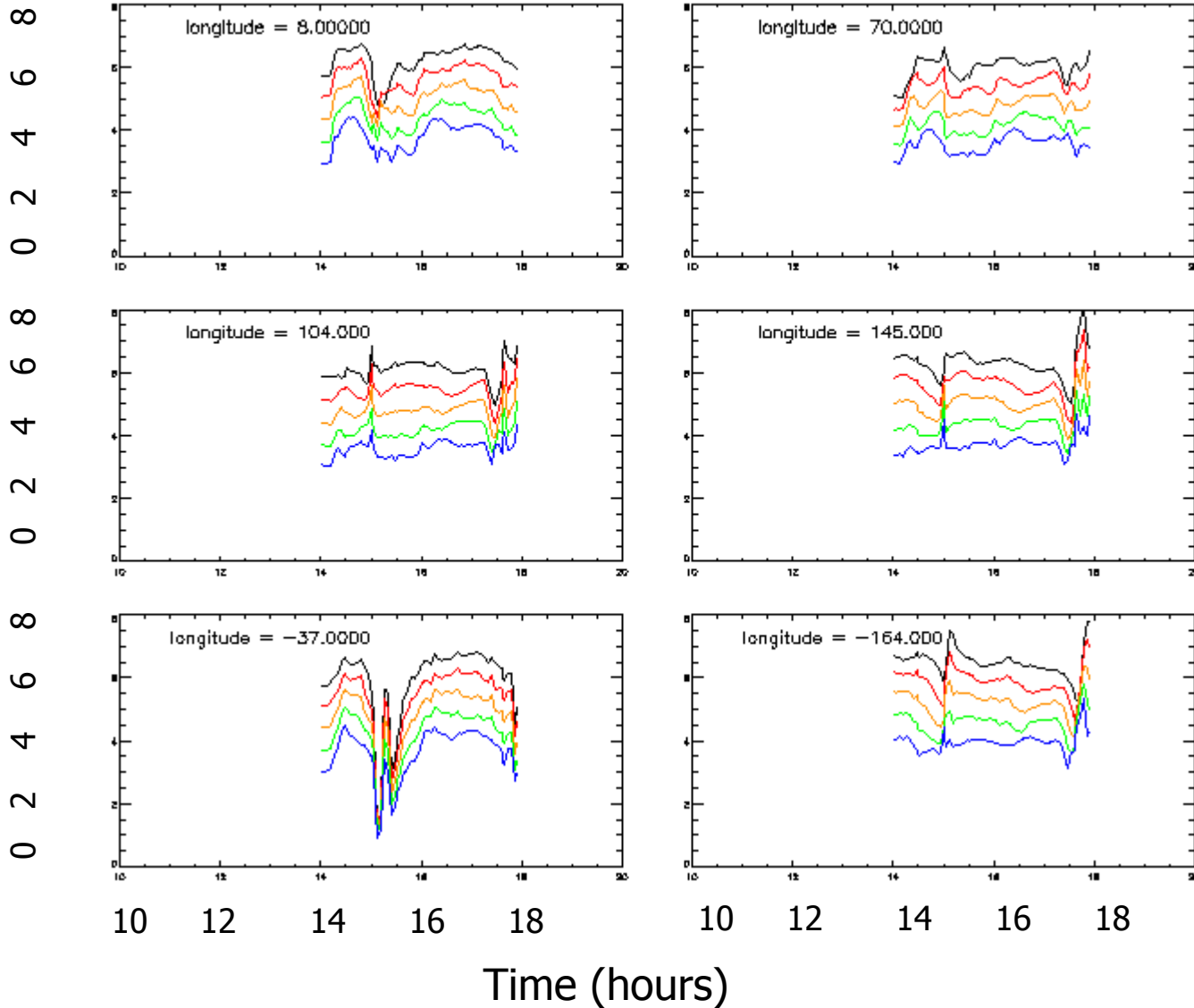
Simulated Solar Wind Data

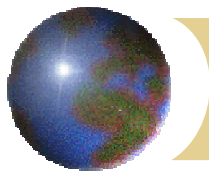




Geosynchronous Plots

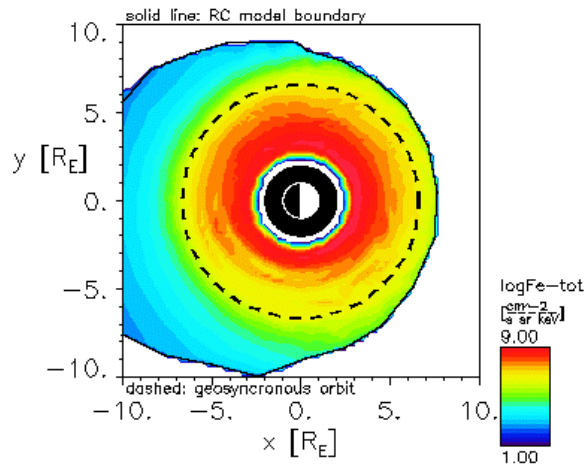
Log(Electron Flux (#/cm²/s/sr/keV))



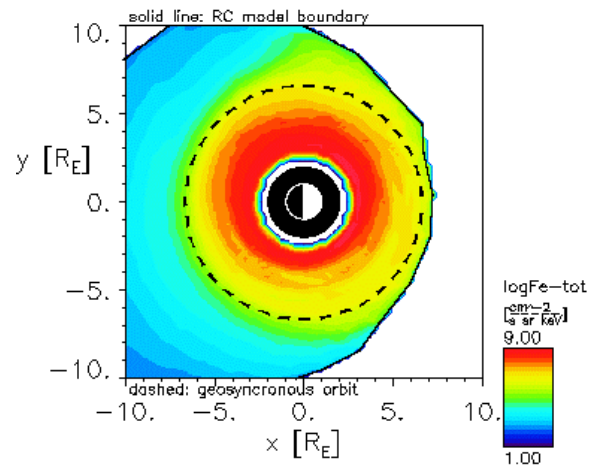


Equatorial Plane Plots

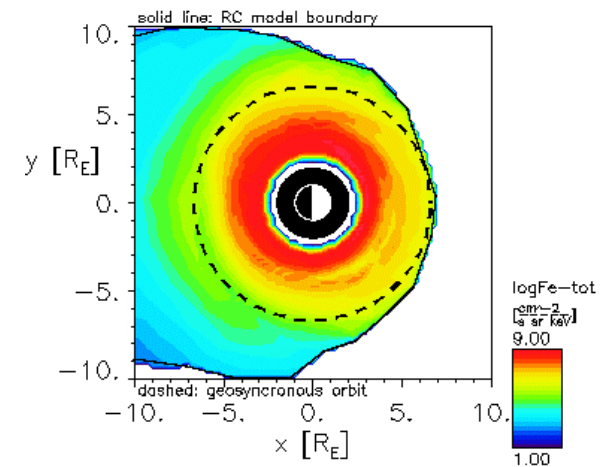
03/21/2002 Time = 17:16:01 En. = 62.5keV



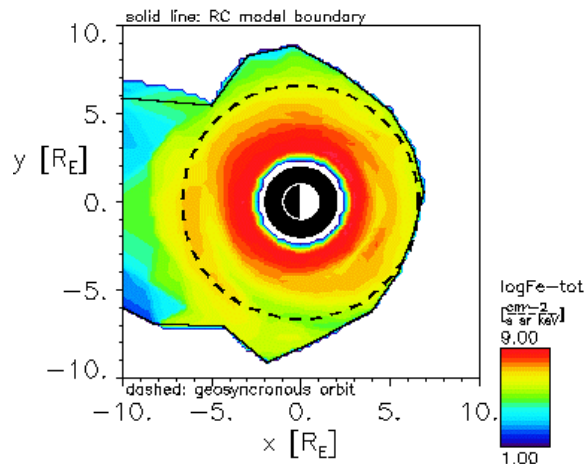
03/21/2002 Time = 17:24:00 En. = 62.5keV



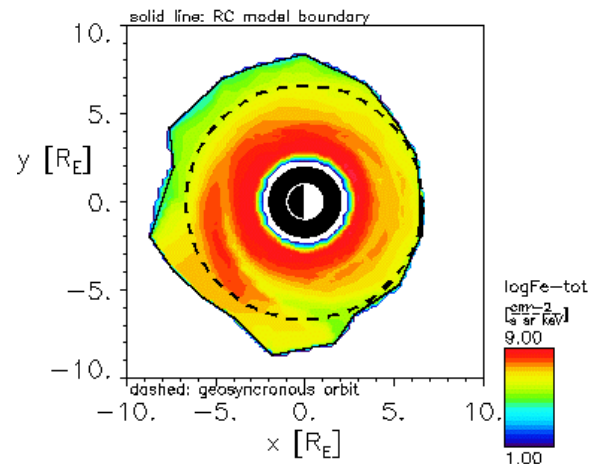
03/21/2002 Time = 17:31:59 En. = 62.5keV



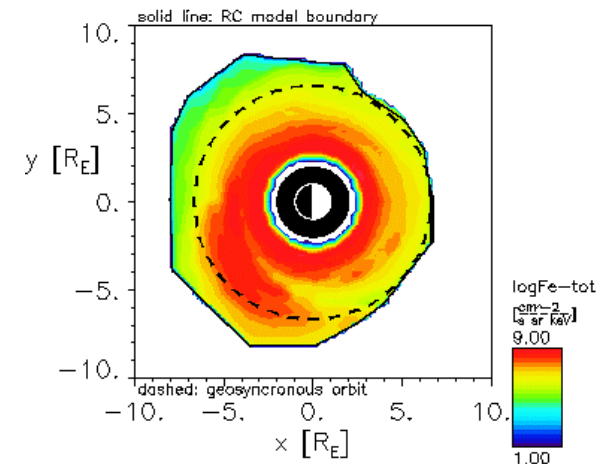
03/21/2002 Time = 17:40:01 En. = 62.5keV

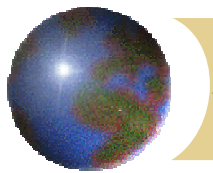


03/21/2002 Time = 17:43:59 En. = 62.5keV



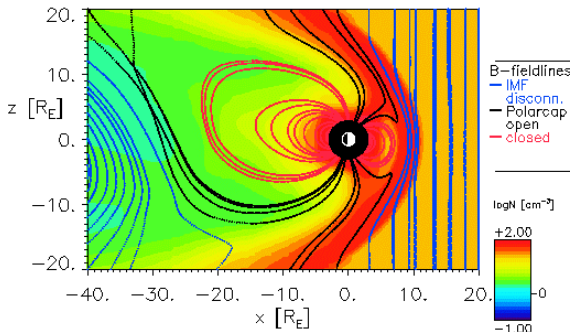
03/21/2002 Time = 17:48:00 En. = 62.5keV



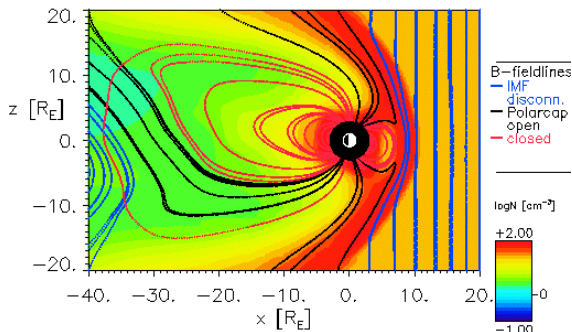


Magnetospheric Plots

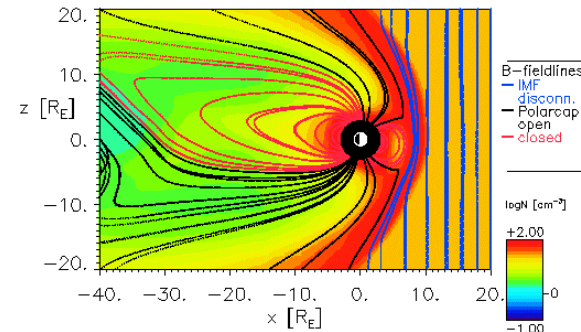
03/21/2002 Time = 17:16:00 $y = 0.00R_E$



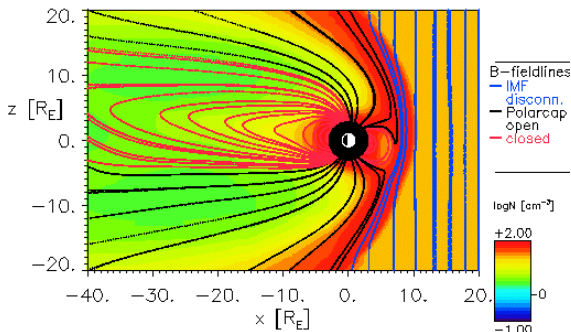
03/21/2002 Time = 17:20:00 $y = 0.00R_E$



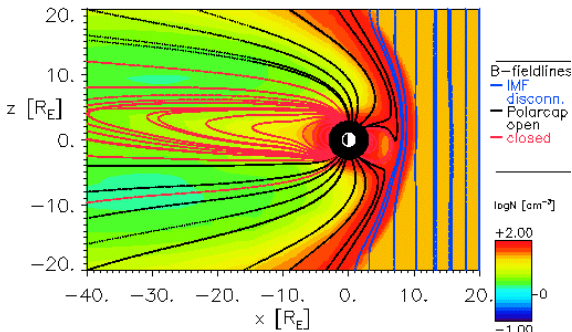
03/21/2002 Time = 17:24:00 $y = 0.00R_E$



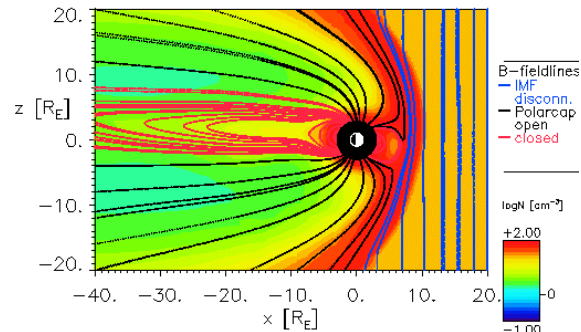
03/21/2002 Time = 17:28:00 $y = 0.00R_E$



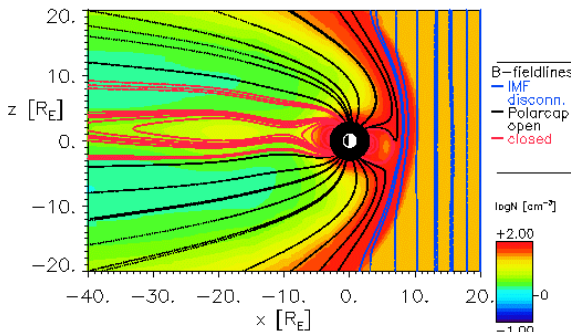
03/21/2002 Time = 17:32:00 $y = 0.00R_E$



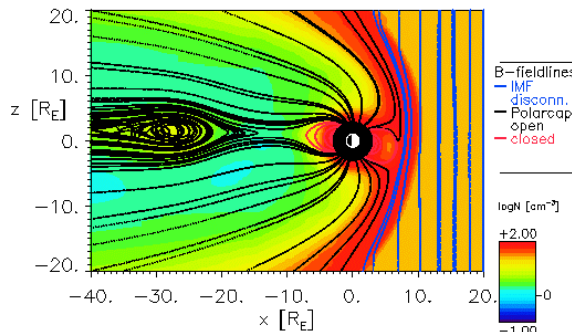
03/21/2002 Time = 17:36:00 $y = 0.00R_E$



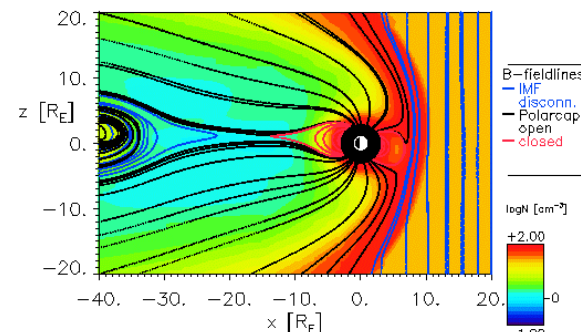
03/21/2002 Time = 17:40:00 $y = 0.00R_E$

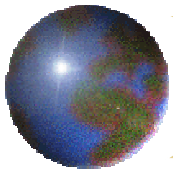


03/21/2002 Time = 17:44:00 $y = 0.00R_E$

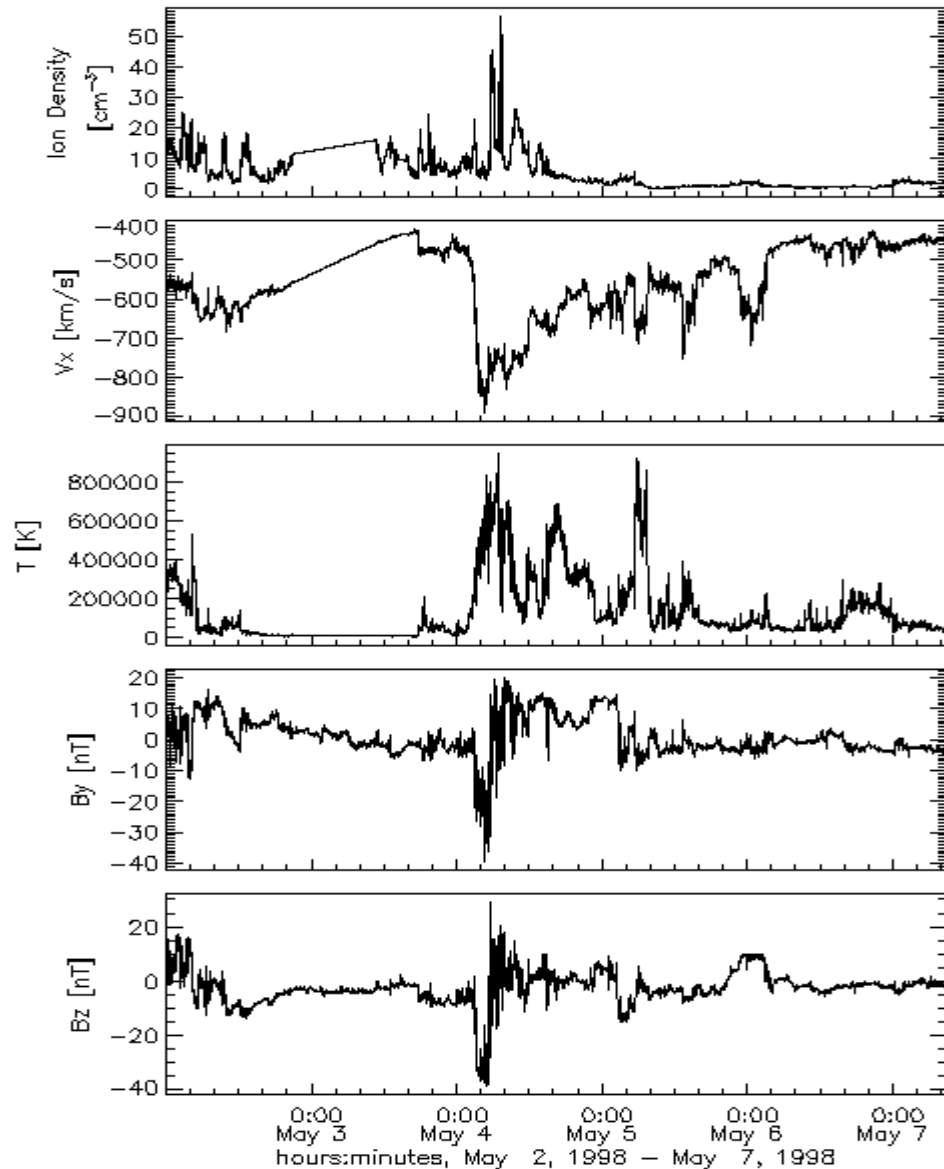


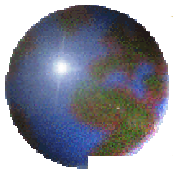
03/21/2002 Time = 17:48:00 $y = 0.00R_E$





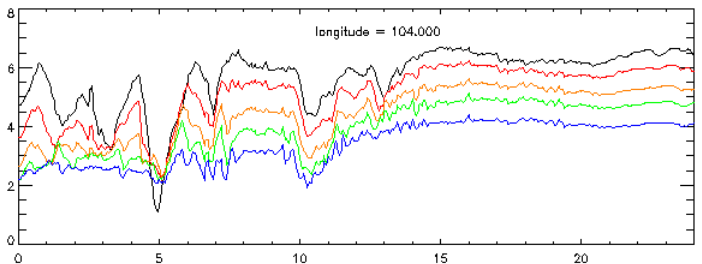
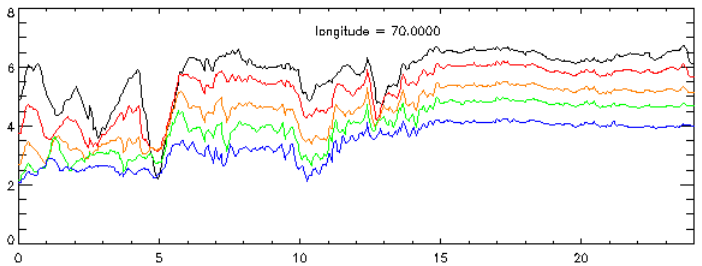
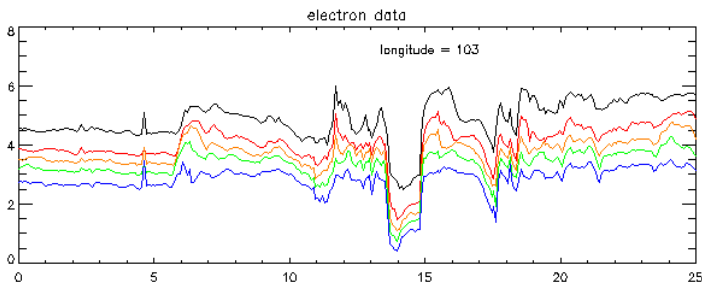
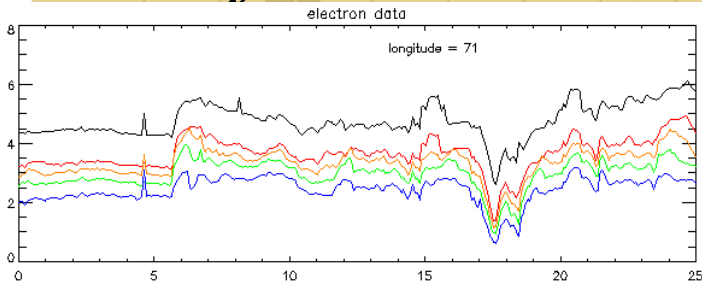
Solar Wind Data May 2-6, 1998





May 2, 1998 Ring Current Results

Log(Electron Flux (#/cm²/s/sr/keV))



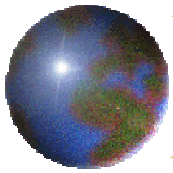
Time (hours)

LANL data for May 2, 1998

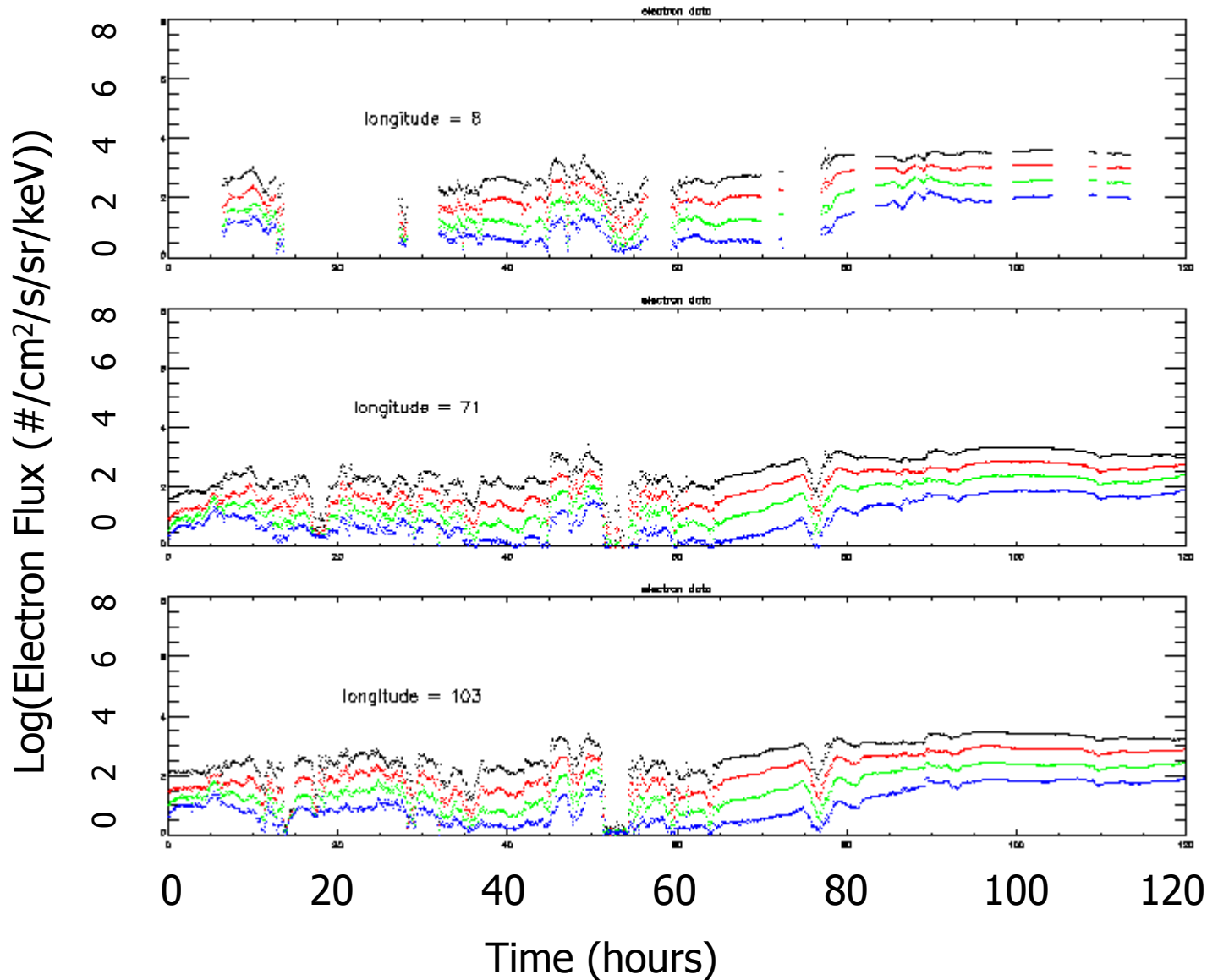
Black: 50-75keV
Red: 75-105keV
Orange: 105-150keV
Green: 150-225keV
Blue: 225-315keV

Model results for May 2, 1998

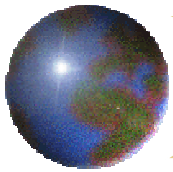
Black: 62.5 keV
Red: 90 keV
Orange: 137.5 keV
Green: 187.5 keV
Blue: 270 keV



May 2-6, 1998 LANL Data

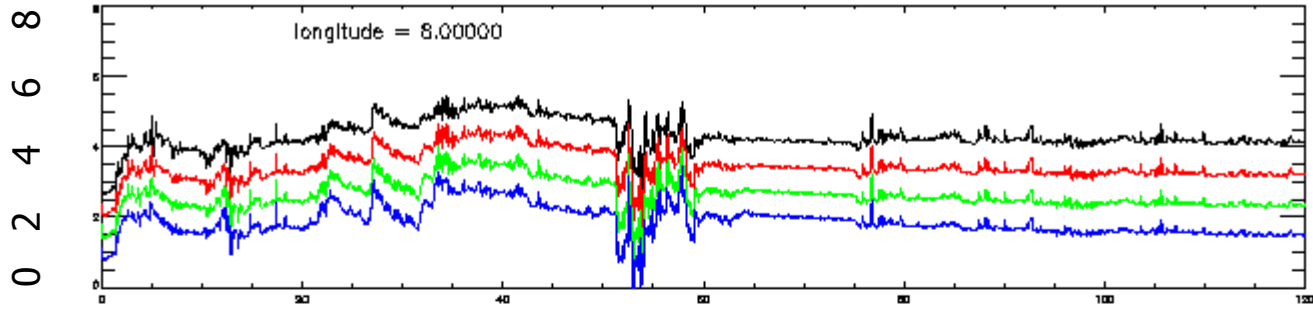


Black: 315-500 keV
Red: 500 - 750 keV
Green: .75 - 1.1 MeV
Blue: 1.1 - 1.5 MeV

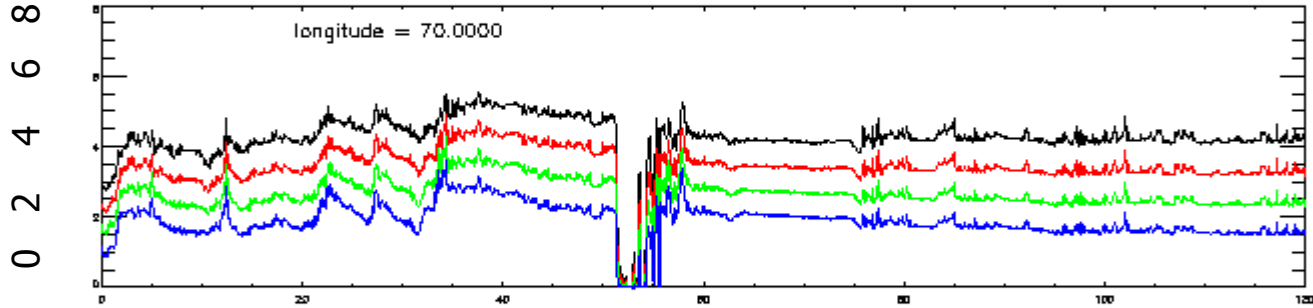


May 2-6, 1998 Model Results

Log(Electron Flux (#/cm²/s/sr/keV))

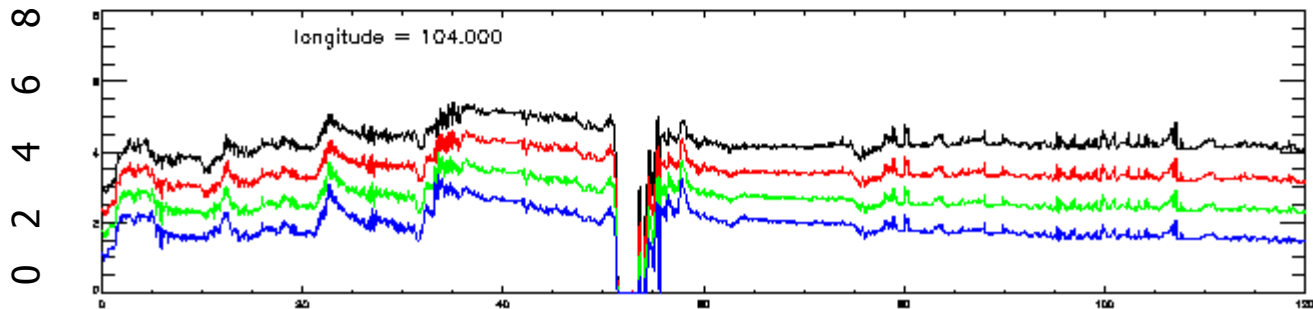


Black: 407.5 keV
Red: 625 keV
Green: .925 MeV
Blue: 1.3 MeV



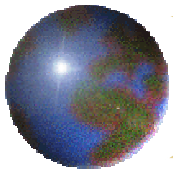
Radiation
Belt Model

MHD
boundary



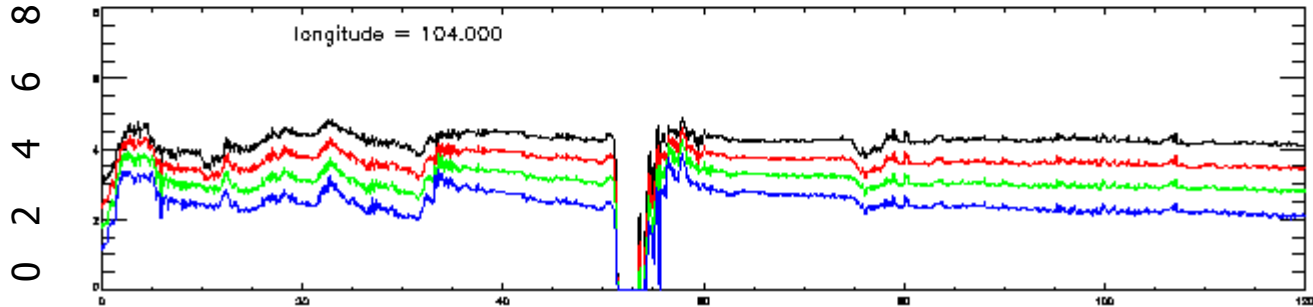
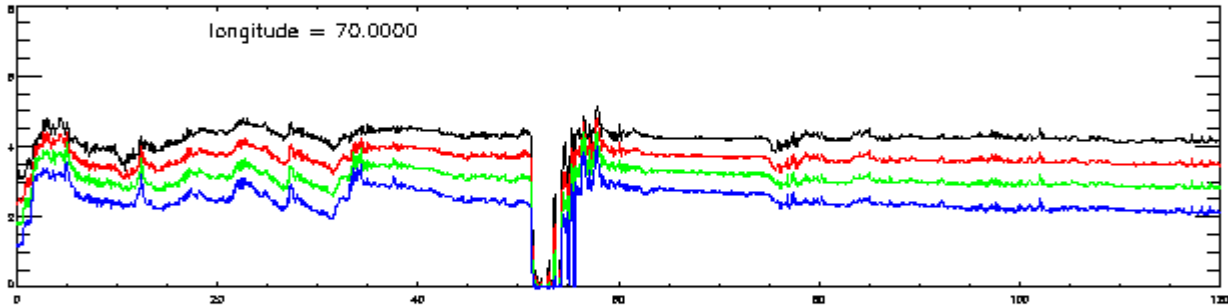
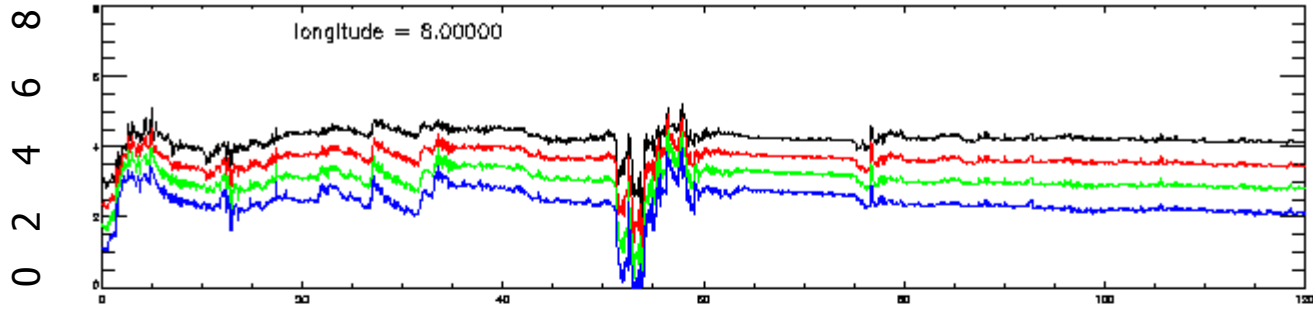
0 20 40 60 80 100 120

Time (hours)



May 2-6, 1998 Model Results

Log(Electron Flux (#/cm²/s/sr/keV))

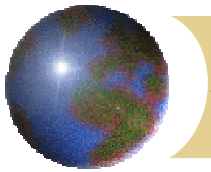


Time (hours)

Black: 407.5 keV
Red: 625 keV
Green: .925 MeV
Blue: 1.3 MeV

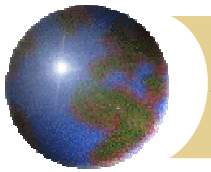
Radiation
Belt Model

Empirical
boundary



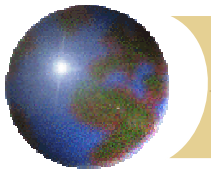
Radiation Belt Comparison

- For both the empirical and BATSRUS MHD boundary, the magnitudes of the electron flux are higher than the observed flux levels in the data at the beginning of the run.
- The magnitudes of the fluxes are closer to the data during the recovery phase but still higher than the data.
- Between 20 and 35 hours, both the model and the data see a decrease in the flux. There are other flux decreases that are seen in the
- The models are missing the flux increase from 60 to 80 hours. The model does not have an energy diffusion term to account for interaction with waves.



Conclusions

- Using real solar wind data, the ring current is mainly driven by changes in ionospheric potential.
- During these events, flux dropouts are not seen and injections tend to be smaller.
- Using simplified solar wind, dipolarization in the tail magnetic field can be seen in the MHD model. During dipolarization, the ring current model does show flux dropouts and larger injections.
- The magnitude of the fluxes tend to be higher than the data in both the ring current and radiation belt models.
- The model is missing the flux increase seen in the data during storm recovery.



Future Work

- ➊ Better resolution in the MHD simulation in the tail region will allow better resolution of thin current sheets and may improve the ring current and radiation belt simulation.
- ➋ The contribution of the radial diffusion term to changes in energy is small compared with other terms. Additional testing of the diffusion term is required.
- ➌ Addition of an energy diffusion term in the radiation belt will allow better modeling of the recovery phase of the storm.